Large aperture, highly uniform narrow bandpass Fabry Perot filter using photosensitive As 2 S 3 thin films

Antoine Bourgade, Julien Lumeau

Large aperture, highly uniform narrow bandpass Fabry Perot filter using photosensitive As_2S_3 thin films

ANTOINE BOURGADE AND JULIEN LUMEAU*

Aix Marseille Univ, CNRS, Centrale Marseille, Institut Fresnel, Marseille, France
**Corresponding author: julien.lumeau@fresnel.fr*

Received XX Month XXXX; revised XX Month, XXXX; accepted XX Month XXXX; posted XX Month XXXX (Doc. ID XXXXX); published XX Month XXXX

We present a thorough study of the use of As_2S_3 thin films for the fabrication of high performance bandpass filters. We show that these layers can be included inside a multilayer Fabry-Perot structure in order to produce large aperture narrowband pass filters. These layers can also exhibit large local refractive index change up to 0.1 when they are exposed to actinic radiation at 470 nm. Kinetics of photosensitivity are presented. We show that these effects can then be implemented to locally modify the spectral performance of a Fabry-Perot filter after deposition. Highly uniform 65×60 mm² filters with 4 nm bandpass at 800 nm and ±0.1% fluctuations of the central wavelength are demonstrated using this technique. © 2018 Optical Society of America

***OCIS codes**: (160.5335) Photosensitive materials; (310.6845) Thin film devices and applications*

http://dx.doi.org/10.1364/OL.99.099999

For the past couple of decades, there has been very large progress within the fabrication method and the complexity of optical thin film filters. Coatings can now be accurate at nanometric scales even for stacks up to hundreds of layers. However, more and more uniform and performant filters are now needed, requiring better and better control of the processes during the deposition. Spectral performances of a filter are related to the optical thickness of each layer and performances are fixed at filter achievement. Moreover, due to variations of the deposited thickness over the substrate aperture, the performances of the filters vary accordingly. This problem is particularly important in case of narrow bandpass filters. Actually, it can be shown [1] that the relative variation of the central wavelength (λ) of a bandpass filter is directly related to the relative variation of the thickness (nt) of its cavity:

$$\frac{\Delta\lambda}{\lambda} = \kappa \frac{\Delta nt}{nt} \quad (1)$$

Where κ is a factor taking into account the phase dispersion derivative of the mirrors that we considered as equal to one in this paper. As of today, the best deposition techniques allow securing a close to 0.1% change of the thickness over a 100 mm aperture [2]. This non uniformity results in variation of the central wavelength of 1 nm for a filter centered at 1 µm. But most of the standard deposition techniques based on evaporation by sputtering are generally resulting in uniformities within the 1%-range such as it is not possible to fabricate large aperture filters with bandwidth smaller than 10 nm.

In this paper, we propose to overcome this limitation by using materials which optical thickness can be changed after deposition. The concept of such an approach was introduced some time ago [3] and basic proof-of-concept was published about 10 years ago [4]. This approach relies on the fabrication of bandpass filters made of photosensitive materials in order to locally correct the central wavelength of the filter using photo-induced refractive index change. However, in ref. [4], only small 5×5 mm² uniform bandpass filter was demonstrated. In this paper, we present a thorough analysis of the fabrication of large aperture narrowband pass filters at 800 nm. We first present a characterization of the photosensitivity of thin As_2S_3 films and then the use of this material for the fabrication of high performance bandpass Fabry-Perot filter. We then present a method for automatic local correction of a bandpass filter and demonstrate a highly uniform 60×60 mm²-square filter with 5 nm bandpass and ±0.1% fluctuations of the central wavelength.

For the development and manufacturing of photosensitive optical thin films, we used chalcogenide glasses such as As_2S_3 also known as AMTIR-6. This glass is known for its broad transparency in the near and far infrared (AMTIR stands for Amorphous Material Transmitting Infrared Radiations) and has the unique characteristic of being photosensitive, i.e. some of its opto-geometrical properties can be modified after exposure to actinic radiation. This characteristic has already been demonstrated in linear regime [5,6] and non-linear one (two photons absorption) [7]. In previous research, it has been shown that the photo-induced refractive index change can go up to 0.016 [8]. Many applications have also been demonstrated with such a material including waveguides for example [5,9]. This material and its photosensitivity has also been used to create gratings and lenslets on the surface of those films with above band gap illumination [10,11]. But, to the best of our knowledge, no optical quality coatings compatible with the manufacturing of complex optical

elements have ever been fabricated. The chalcogenide layers and thin film stacks were produced using electron beam deposition in a Bühler SYRUSpro710 machine. The whole deposition was monitored by optical monitoring using a Bühler OMS 5000 system and deposition rate was controlled with quartz-crystal monitoring system. The material used to deposit is a bulk amourphous As_2S_3 glass blank. The residual pressure inside the vacuum chamber was around ~10^{-6} mbar, and the deposition rate was set to 3Å/s. The chalcogenide layers were fabricated using electron beam deposition while the Bragg mirrors of the Fabry Perot Filter (made with alternated Nb_2O_5 and SiO_2 layers) were fabricated using plasma assisted electron beam deposition. Due to the photosensitive nature of such a material, we protected the samples from any ambient light exposure by keeping them in dark boxes, except during the exposure process.

To characterize the photosensitive properties of the As_2S_3 layers, we deposited 990 nm thick (3λ/2 at 1550 nm) single layers. Then, using a Perkin Elmer Lambda 1050 spectrophotometer, we measured the spectral dependence of the transmission before and after exposing the layer to a 20 mW LED at 470 nm (Figure 1). One can see that after exposing the layer with a dosage of 110 J/cm^2, the transmission spectrum is shifted to longer wavelengths by 3.5% and the amplitude of the intensity modulation is also increased by 6.4%. Reverse engineering on these two curves [12] allows to show that at 800 nm, the refractive index is changed from 2.412 to 2.497 without any change of the layer thickness.

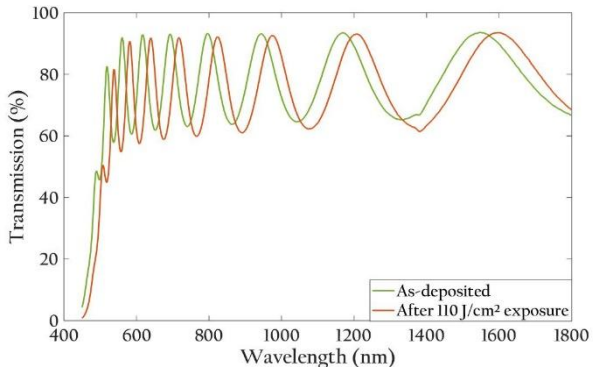

Fig. 1: Evolution of the spectral dependence of the transmission of a 990 nm thick As2S3 layer (green: as deposited layer and red:layer after exposure to a 20 mW LED at 470 nm).

To better characterize the refractive index change kinetics, we then exposed the As_2S_3 layer with different dosages, measured the spectral dependence of the transmission and reflection after each dosage increment and finally implemented a reverse engineering technique to extract the opto-geometrical parameters of the layer. Figure 2 shows the evolution of the refractive index change in As_2S_3 layer for exposure dosage from 0 to 110 J/cm^2. A refractive index increment as large as 0.08 at 800 nm can be induced with a dosage of ~20 J/cm^2. For larger dosages, a saturation of the refractive index is observed. In addition, it is worth noting that no change of the layer thickness could be detected with our reverse engineering method and this was confirmed by optical profilometer measurements. Finally, the observed refractive index changes are non-reversible and stable (at least for more than 12 months – time since we started this work) at room temperature.

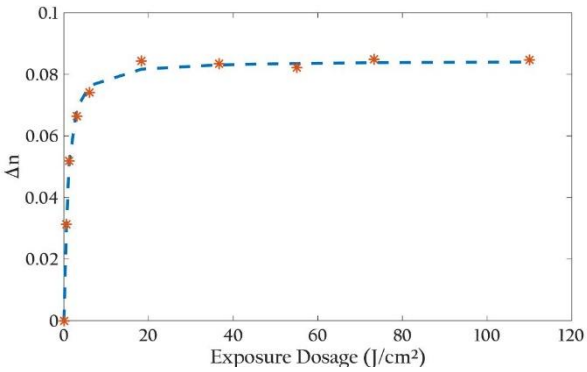

Fig. 2: Evolution of the refractive index change as a function of the exposure dosage at 470 nm.

We then analyzed how the As_2S_3 layer can be integrated within a multilayer structure. We designed a narrow bandpass filter centered at 800 nm with a single cavity Fabry-Perot structure, i.e. composed of one As_2S_3 cavity separated by two dielectric quarter wave layer-based mirrors. The materials used for the mirrors are silica (SiO_2) as low index material and niobia (Nb_2O_5) as high refractive index material. The design of the filter is:

$$(HL)^4 \ / \ 4\ ChG \ / \ (LH)^4 \qquad \textbf{(2)}$$

where H stands for a quaterwave Nb_2O_5 layer, L for a quaterwave SiO_2 layer and ChG for a quaterwave As_2S_3 layer. Such a filter generates a narrow bandpass with a Full Width at Half Maximum (FWHM) of 4 nm. A prototype of this filter was fabricated within our technological platform on a 4-inch diameter glass substrate.

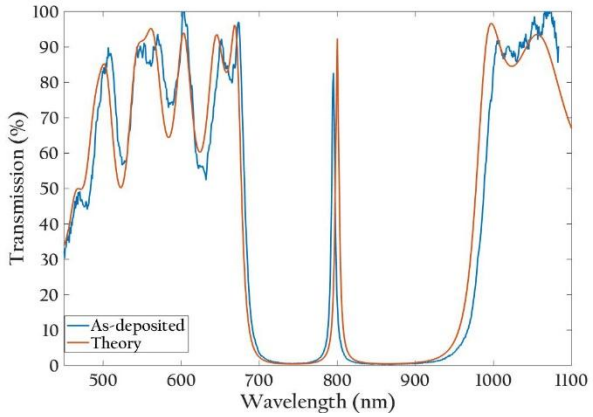

Fig. 3: Spectral dependence of the transmission of a $(HL)^4$ / 4 ChG / $(LH)^4$Fabry Perot filter. Theoretical filter: red curve, experimental filter: blue curve.

After deposition, the filter was characterized with a Perkin Elmer Lambda 1050 spectrophotometer between 450 and 1100 nm. In Figure 3, we overlapped the measured (blue curve) and theoretical (red curve) spectral dependence of the transmission of the filter. One can see that the overall experimental transmission curve is very similar to that was theoretically calculated. However, one can see that the central wavelength is blue shifted while the side of the mirrors are red-shifted. This observation shows that the

cavity was not perfectly matched during the fabrication. In addition, as the optical monitoring was done on a separate test glass, this error might also be due to inherent non-uniformity of the deposition. Indeed, it is well known that the thickness of the deposited layers will vary over the filter aperture resulting in a variation of the spectral performance. Such effect becomes noticeable and non-negligible with 4-inch diameter filters. In order to characterize this uniformity, we developed a dedicated optical setup (Figure 4). It is composed with a collimated white-light source. The 1 mm square beam is sent to the filter to be characterized and the transmitted beam is then collected within a second fiber, sent to a Wasatch Photonics VIS-NIR spectrometer and analyzed within the [400-1100] nm spectral range with a 0.6 nm spectral resolution. The sample is placed on two translation stages in order to scan the local transmission of the filter.

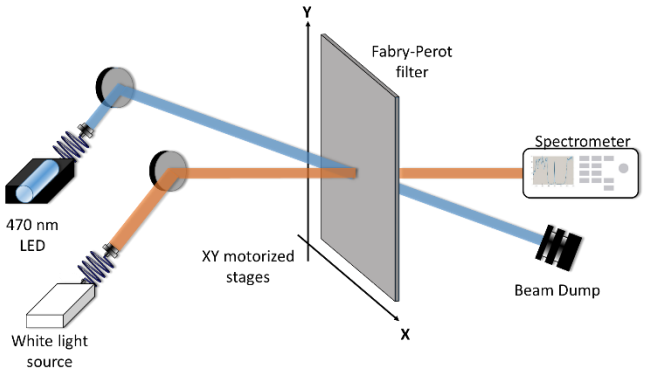

Fig. 4: Scheme of the pump/probe experimental setup used to both characterize the local spectral performances in transmission of the filter and correct the local central wavelength of the filter.

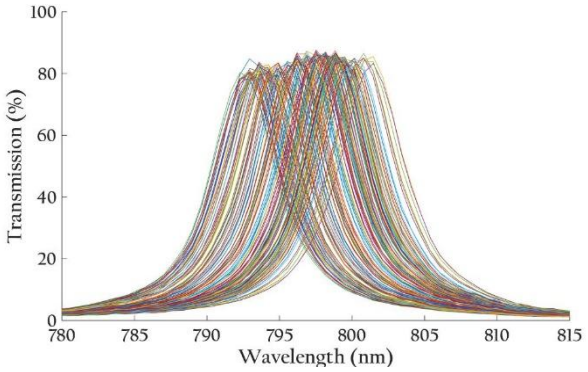

Fig. 5: Evolution of the spectral dependence of the transmission measured on a Fabry-Perot filter. Each curve was measured on a 1 mm^2 spot size over a 65x60 mm^2 aperture

The local spectral dependence of the transmission was measured over 1800 1 mm^2 regions on a 65×60 mm^2 aperture. We then plotted in Figure 5 an overlay of the measured transmission curves within the bandpass region. One can see that the filter is centered around 800 nm but the central wavelength shows some variations up to 9.2 nm, i.e. 1.1% variation of the central wavelength over the filter aperture. This dispersion illustrates the non-uniformity of the SYRUSpro machine and is within the expected performances with such a deposition system. Such a dispersion of the central wavelength makes this filter not usable over its whole aperture as the summing of the spectral performance over its aperture will result in deteriorated spectral performances. In this work, we implemented a similar approach to that was presented by Shen et al. [13]. However, in order to demonstrate that this technique is reliable and predictable, we developed a pump/probe system that allowed automatic correction of the filter for each of the 1800 measured points (Figure 4). Indeed, we added to the spectrophotometric system (probe system) an exposure system (pump system) composed with a blue LED of 20 mW emitting at 470 nm. This exposure system produces a 1 mm square spot that perfectly overlaps the transmission measurement spot.

Then, at first, we characterized the kinetics of central wavelength change versus exposure dosage on a single point. Dosage was increased up to 110 J/cm^2 with a 5 J/cm^2 step and the transmission spectrum was measured after each of these steps. By increasing the dosage, the central wavelength of the filter is red-shifted but no change of the transmission could be detected (within the precision of the measurement (±1%), confirming that the refractive index change does not induce losses within the layer. We plotted in Figure 6 the evolution of the central wavelength as a function of the dosage. We can clearly see that the evolution of the central wavelength is similar to that of refractive index change that was measured in As_2S_3 single layers. The kinetics are however different (4 times decrease) as the electric field distribution within the cavity at 470 nm induces a decrease of the local effective exposure dosage. A maximum change of the central wavelength of +10 nm, i.e. 1.2% can be induced with this technique. This value is therefore large enough to be able to locally correct each of the measured spectrum and make the filter uniform.

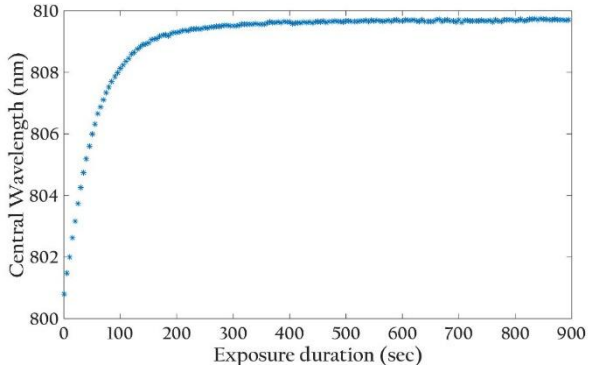

Fig. 6: Dependence on dosage of the central wavelength peak

To achieve very uniform filter, we decided to center the whole filter at 801 nm with a precision of 0.1%, i.e. 10 times better than the original one. In this case, only red-shift of the filter is necessary. This case is not a limited case since if a more specific wavelength would be needed, it could be possible to adjust the fabrication procedure to guaranty that the part of the filter that has the largest central wavelength is below that targeted one. We developed a LabVIEW program that allows to sequentially measure the local transmission, expose the sample at 470 nm and then measure the transmission again and repeating this procedure until the value of 801 ±0.8 nm (i.e. compatible with the maximum measured central

wavelength on the filter) is achieved. This procedure is then repeated for each of the 1800 points.

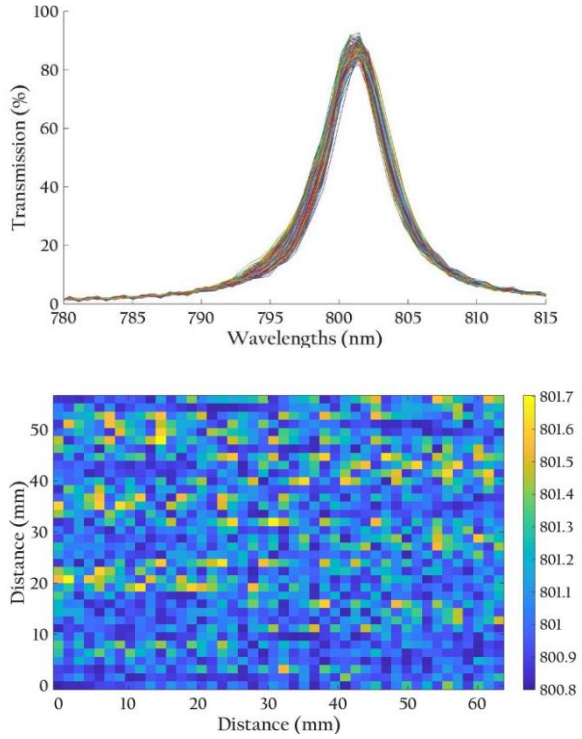

Fig. 7: (On the left) spectral dependence of the transmission measured on each 1mm^{2}spot over a 65x60 mm^2 aperture after correction of the filter. (On the right) Mapping of the central wavelength of the filter after correction

After this point-by-point correction of the local transmission of the filter, we plotted in Figure 7 the evolution of the central wavelength of the filter over its aperture as well as an overlay of the measured transmission spectra after correction. The variations of the central wavelength of the filter over its aperture are now 10 times lower (going from 800.8 nm to 801.7 nm) than before correction. Using this technique, the central is controlled with a ±0.05% precision range over a 65 × 60 mm^2 aperture. This value is equal, if not better than what can be achieved with highly uniform deposition machines [2]

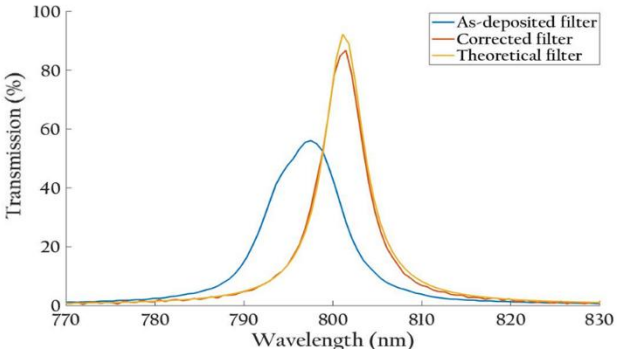

Fig. 8: Behavior of the filter using a large beam (50mm diameter beam)

In order to confirm that the filter can now be used in full aperture, we modified the set-up in Figure 4 and expanded the illuminating beam to a diameter of 50 mm. The collecting collimator was also adapted in order to be able to collect, in the spectrometer, the whole transmitted beam and therefore be able to characterize the average transmission spectrum. This measurement was carried out before and after correction of the filter and was compared to the theoretical transmission of the filter (Figure 8). Theoretically, the filter is expected to have a FWHM of 4 nm and a maximum transmission of 92%. The as-deposited filter presents a FWHM of ~10 nm and a maximum of transmission of ~50%. These deteriorated performances are due to the fact that with a large beam, the measured transmittance is the average of the transmission spectra over the filter aperture. Due to the non-uniformity which is 2.5× the FWHM, both the FHWM and the transmittance are highly affected. After correction, the variation of the central wavelength has been decreased by 10 times and is now only 0.25× the FWHM. The transmission of the filter becomes much closer to the theoretical one, i.e. we have the FWHM = 5 nm and the maximum transmittance = 85%).

We have shown in this letter the possibility to correct, after deposition, the local non-uniformity of narrow bandpass filters. This correction relies on the use of photosensitive As_2S_3 layers that are used as cavities in Fabry Perot structures. Using a relative refractive index change equal to the relative thickness change (due to non-uniformity issues) and with opposite sign, it is possible to generate highly uniform large aperture bandpass filters. We have shown a method that automatically corrects for the non-uniformity of a filter. Example of a 5 nm FWHM filter centered at 801 nm with deviation of the central wavelength less than 0.1% over 65×60 mm^2 squared aperture has been demonstrated. These results pave a way to the fabrication of large aperture, highly uniform, filters with more complex structures.

Funding. Ministry for armed Forces (DGA) and Aix-Marseille Université.

References

1. M. Lequime, R. Parmentier, F. Lemarchand and C. Amra, Appl. Opt., 41, 3277-3284 (2002)
2. T. Begou, H. Krol, D. Stojcevski, F. Lemarchand, M. Lequime, C. Grezes-Besset and J. Lumeau, CEAS Space J 9(4), 2017.
3. M. Lequime and J. Lumeau, Advances in Optical Thin-Films (Jena, Germany), invited talk, paper 5963-08, September 2005
4. W.D. Shen, M. Cathelinaud, M. Lequime, V. Nazabal, and X. Liu, Opt. Commun., 281, 2008
5. H. Hisakuni and K. Tanaka, Solid State Communications, Vol. 90, No. 8, 1994
6. K. Tanaka, N. Toyosawa, and H. Hisakuni, Opt Lett., Vol. 20, No. 19, October 1, 1995
7. C. Meneghini and A.Villeneuve, J. Opt. Soc. Am. B, Vol. 15, No. 12, December 1998.
8. J. Hu, M. Torregiani, F. Morichetti, N. Carlie, A. Agarwal,et al, Opt Lett., Vol. 35, No. 6 , March 15, 2010
9. R. Vallée, S. Frédérick, K. Asatryan,M. Fischer, T. Galstian, Opt Commun., Vol 230, No 4-6, Feb. 2004
10. S. Ramachandran, S.G. Bishop, J.P. Guo, et D.J. Brady, IEEE Photonics Technology Letters 8, No 8, August 1996

11. H. Hisakuni and K. Tanaka, Opt. Lett., vol. 20, No 9, 1995.
12. L. Gao, F. Lemarchand, M. Lequime Journal of the European Optical Society : Rapid publications, European Optical Society, 8, 2013
13. W.D. Shen, M. Cathelinaud, M. Lequime, F. Charpentier, and V. Nazabal, Opt. Express, 16, 2008

Full References:

1. Michel Lequime, Remy Parmentier, Fabien Lemarchand, and Claude Amra, "Toward tunable thin-film filters for wavelength division multiplexing applications," Appl. Opt. 41, 3277-3284 (2002)
2. T. Begou, H. Krol, D. Stojcevski, F. Lemarchand, M. Lequime, C. Grezes-Besset and J. Lumeau, "Complex optical interference filters with stress compensation for space applications", CEAS Space J 9(4), 441–449 (2017).
3. M. Lequime and J. Lumeau, "Laser trimming of thin-film filters", Advances in Optical Thin-Films (Jena, Germany), invited talk, paper 5963-08, September 2005
4. W.D. Shen, M. Cathelinaud, M. Lequime, V. Nazabal, and X. Liu, "Photosensitive post tuning of chalcogenide Te20As30Se50 narrow bandpass filters," Opt. Commun., 281, 3726-3731 (2008)
5. H. Hisakuni and K. Tanaka, “Laser-induced persistent self-focusing in As2S3 glass”, Solid State Communications, Vol. 90, No. 8, pp. 483-486, 1994
6. K. Tanaka, N. Toyosawa, and H. Hisakuni “Photoinduced Bragg gratings in As2S3 optical fibers”, Optics Letters, Vol. 20, No. 19, October 1, 1995
7. C. Meneghini and A.Villeneuve, “As2S3 photosensitivity by two-photon absorption: holographic gratings and self-written channel waveguides”, J. Opt. Soc. Am. B, Vol. 15, No. 12, December 1998.
8. J. Hu, M. Torregiani, F. Morichetti, N. Carlie, A. Agarwal,et al., “Resonant cavity-enhanced photosensitivity in As2S3 chalcogenide glass at 1550 nm telecommunication wavelength”, Optics Letters, Vol. 35, No. 6 , March 15, 2010
9. R. Vallée, S. Frédérick, K. Asatryan,M. Fischer, T. Galstian, “Real-time observation of Bragg grating formation in As2S3 chalcogenide ridge waveguides”, Optics Communications, Vol 230, No 4-6, pp.301-307, Feb. 2004
10. S. Ramachandran, S.G. Bishop, J.P. Guo, et D.J. Brady. « Fabrication of holographic gratings in As2S3glass by photoexpansion and photodarkening ». IEEE Photonics Technology Letters 8, n° 8 (august 1996): 1041‑ 43
11. H. Hisakuni and K. Tanaka, “Optical fabrication of microlenses in chalcogenide glasses,” Opt. Lett., vol. 20, pp. 958-960, 1995
12. Gao, L., F. Lemarchand, & M. Lequime. "Refractive index determination of SiO2 layer in the UV/Vis/NIR range: spectrophotometric reverse engineering on single and bi-layer designs." Journal of the European Optical Society - Rapid publications [Online], 8 (2013)
13. W.D. Shen, M. Cathelinaud, M. Lequime, F. Charpentier, and V. Nazabal, "Light trimming of a narrow bandpass filter based on a photosensitive chalcogenide spacer," Opt. Express, 16, 373-383 (2008)